

# Hydrogen migration in diamond-like carbon films

E. Vainonen,<sup>a)</sup> J. Likonen,<sup>b)</sup> T. Ahlgren, P. Haussalo, and J. Keinonen  
*Accelerator Laboratory, P.O. Box 43, FIN-00014 University of Helsinki, Finland*

C. H. Wu

*The NET Team, Max-Planck-Institut für Plasmaphysik, Boltzmannstrasse 2, D-85748 Garching bei München, Germany*

(Received 8 May 1997; accepted for publication 8 July 1997)

Properties of physical vapor deposited diamondlike carbon (DLC) films and the migration of hydrogen in  $H^+$  and  $^4He^+$  ion implanted and hydrogen co-deposited DLC films have been studied. Measurements utilizing Rutherford backscattering spectrometry showed that the films studied have an average mass density of  $2.6 \pm 0.1 \text{ g/cm}^3$ . The bonding ratio  $sp^3/sp^2$  is typically 70% measured with the electron spectroscopy for chemical analysis technique. Impurities and their depth distributions were deduced from the particle induced x-ray emission and secondary ion mass spectrometry (SIMS) measurements. Distributions of implanted and co-deposited hydrogen were measured by the nuclear resonance reaction  $^1H(^{15}N, \alpha\gamma)^{12}C$  and SIMS. It was found that annealing behavior of implanted H in DLC has a diffusion like character. The obtained diffusion coefficients resulted in the activation energy of  $2.0 \pm 0.1 \text{ eV}$ . It was observed that in H co-deposited DLC films the temperature of H release varied between 950 and 1070 °C depending on the H concentration.

© 1997 American Institute of Physics. [S0021-8979(97)04120-0]

## I. INTRODUCTION

Carbon is one of the elements in the periodic table, which exists in different allotropic forms such as graphite, amorphous carbon, glassy carbon, diamond, fullerene and other stable clusters. The unique properties of the carbon allotropic forms make them suitable for different applications, among which fusion devices are of great interest. Carbon materials have been widely used as plasma facing components in tokamak fusion devices because of their excellent thermal properties. Diamondlike carbon (DLC) films or carbon based composite films are planned to be used as divertor material in the next generation fusion energy reactor ITER. From this point of view the understanding of the processes which involve hydrogen trapping and retention in DLC films is very important. This reason has resulted in numerous investigations<sup>1-5</sup> focusing on hydrogen transport and release during hydrogenic plasma bombardment of graphite. Intensive studies of natural diamond and diamond films prepared with different techniques have also been done at different laboratories.<sup>6-10</sup>

In this work, which is a part of the European Union fusion energy research program, we have studied properties of physical vapor deposited (PVD) DLC films and the migration of hydrogen in  $H^+$  and  $^4He^+$  ion implanted and hydrogen co-deposited DLC films. The advantages of the films produced with pulsed arc discharge system are good adhesion to the substrate, high purity and high bonding ratio  $sp^3/sp^2$ . To our knowledge there are no experimental data in the literature on H diffusion in PVD DLC films. By ion implantation the effects of the surface and the surface hydro-

gen diffusion were avoided. Helium implantation was done to investigate the influence of damage on hydrogen retention in the films. This is related to the damage in reactor materials.

## II. EXPERIMENTAL ARRANGEMENTS

DLC films used in this study were made by the company DIARC-Technology Inc. using arc discharge method. The silicon substrate was cleaned by argon etching. Mostly single ionized carbon plasma is generated and accelerated by an arc discharge between a graphite cathode and an anode and directed to the substrate using magnetic filtering. Deposition process takes place in a vacuum (0.1–1 mPa) at room temperature.<sup>11</sup>

The presence of heavy impurities in the DLC films was investigated by the particle induced x-ray emission (PIXE) technique. The measurements were carried out with the external beam of 2.4 MeV protons provided by the 2.5 MV Van de Graaff accelerator of the University of Helsinki. The experimental setup has been described elsewhere.<sup>12</sup> In order to reduce the counting rates from the low energy continuum x rays, an absorber made of five layers of Kapton, each 125  $\mu\text{m}$  thick, was inserted in front of the detector. The counting rate for each run was kept below 1000 cps with 150 nA beam current. Characteristic x rays were detected by a 50  $\text{mm}^2 \times 6 \text{ mm}$  intrinsic Ge detector (Seforad PGP 50-6 OFB) having an energy resolution of 200 eV for the  $FeK_{\alpha}$  peak. The target was positioned at 45° to the incident beam and the detector was placed 10 mm from the sample surface at an angle of 100° to the beam. The spectra were analyzed by the Sampo90 program.<sup>13</sup> X-ray absorption coefficients in Kapton were calculated by using data from Ref. 14.

The analysis of impurities were carried out also by secondary ion mass spectrometry (SIMS) at the Technical Re-

<sup>a)</sup>Corresponding author. Electronic mail: elizaveta.vainonen@helsinki.fi

<sup>b)</sup>Permanent address: Technical Research Centre of Finland, Chemical Technology, P.O. Box 1404, FIN-02044 VTT, Finland.

search Center of Finland. This method resulted in the depth distribution of the impurities. The measurements were done with a double focusing magnetic sector SIMS (VG Ionex IX70S). The current of 5 keV  $O_2^+$  primary ions was typically 400 nA during depth profiling and the ion beam was raster scanned over an area of  $240 \times 430 \mu\text{m}^2$ . Crater wall effects were avoided by using a 10% electronic gate and 1 mm optical gate. The pressure inside the analysis chamber was  $5 \times 10^{-8}$  Pa during the analysis. The depth of the craters was measured by a profilometer (Dektak 3030ST) after SIMS analysis. The uncertainty of the crater depth was estimated to be 5%.

The mass density of the DLC films was investigated by Rutherford backscattering spectrometry (RBS) with 2.7 MeV  $^4\text{He}$  ions obtained from the 2.5 MV Van de Graaff accelerator. Backscattered particles were detected with a 50 mm<sup>2</sup> silicon surface barrier detector placed at a scattering angle of 170°. The counting rate was kept under 1000 cps with the 24 nA beam current. The acceptance solid angle of the detector and the angular divergence of the incident ion beam were confined by slits and apertures to 6.0 mSr and 0.02°, respectively. The spectra were analyzed by the Gisa3.99 program.<sup>15</sup> Non-Rutherford scattering cross sections, needed in an accurate analysis of the 2.7 MeV measurements, are included in the data package of the program.

Three sets of samples were prepared for H migration studies. In the first set samples were implanted with 30 keV  $^1\text{H}^+$  ions. The implantation dose was  $1 \times 10^{16}$  ions  $\text{cm}^{-2}$ . In the second set both 35 keV  $^4\text{He}^+$  and 30 keV  $^1\text{H}^+$  ions were implanted with the implantation dose of  $1 \times 10^{16}$   $\text{cm}^{-2}$  for both ions. The implantation energies were selected to result in same mean ranges (about 250 nm) for both implanted atoms. The implantations were performed at room temperature in the 100 keV isotope separator of the laboratory. In the third set films were grown in H atmosphere. Hydrogen concentration in different depositions was varied by changing the pressure of hydrogen atmosphere between 0.06 and 0.6 mPa.

The isochronal annealings (40 min) were made in a quartz-tube furnace (pressure below 0.05 mPa) at temperatures between 100 and 1100 °C. For SIMS analyses somewhat longer annealing times were used. The annealing regime was 2 h (700 °C), 1 h (800 °C), 40 min (900 and 1000 °C) and 30 min (1100 °C).

For the depth profiling of H atoms the nuclear resonance broadening (NRB) technique with the 6.39 MeV resonance of the  $^1\text{H}(^{15}\text{N}, \alpha\gamma)^{12}\text{C}$  reaction was used.<sup>16</sup> The  $^{15}\text{N}^{2+}$  beam of 150 nA was obtained from the tandem accelerator EGP-10-II of the University of Helsinki. The yield of the 4.43 MeV  $\gamma$  rays from the nuclear reaction was detected as a function of the incident  $^{15}\text{N}$  energy with a large volume ( $2600 \text{ cm}^3$ ) annular bismuth germanate oxide detector protected against the background radiation with a 10-cm-thick lead shield.<sup>17</sup> SIMS experiments with the setup described above for the depth profiling were carried out as well.

The concentration profiles of implanted He and also H atoms were measured by the elastic-recoil-detection-analysis technique.<sup>18</sup> The beam of 25 MeV  $^{16}\text{O}^{5+}$  ions used to bombard the samples was generated by the tandem accelerator.

The angle between the primary beam direction and the target surface was 20°. Recoils were detected by a 50 mm<sup>2</sup> surface barrier detector (Canberra PIPS) centered at an angle of 40° with respect to the incident beam direction. The detector was masked so that it subtended a solid angle of 60  $\mu\text{Sr}$ . A 19- $\mu\text{m}$ -thick mylar absorber foil was used to separate the recoiled H and He atoms and to discriminate the scattered projectile atoms. The accumulated charge was normalized between different measurements by using another 50 mm<sup>2</sup> surface barrier detector located at 170° with respect to the incident beam to count the backscattered beam particles from a tantalum covered, rotating chopper blade.

Electron spectroscopy for chemical analysis (ESCA) was used to characterise the bonding ratio  $\text{sp}^3/\text{sp}^2$  in the DLC films. The analyses were made from the sample surfaces. For a more detailed description of the experimental arrangement and the use of ESCA technique, the reader is referred to an earlier work.<sup>19</sup>

### III. MEASUREMENTS AND RESULTS

Measurements by PIXE and SIMS showed the presence of V, Fe and Ni impurities in DLC films. Further analyses showed that these impurities originate from the graphite used as a cathode in the film preparation. Coatings contained tungsten at the interface between the DLC films and Si substrates. Tungsten was deposited during the etching process of the substrate surface. The thicknesses of layers containing tungsten impurities were obtained in RBS measurements to be 10 nm for films deposited in vacuum and 10–30 nm for H co-deposited films. The W concentration in these layers was obtained to be 0.7 at. %. The total amount of the V, Fe and Ni impurities was obtained to be about 0.12 at. %. This was obtained from PIXE spectra using intensities of x-ray peaks and the tungsten concentration. The values of 570 nm for the thickness of the DLC films deposited in vacuum and 320–422 nm for the H co-deposited films were obtained in SIMS measurements. Measurements by RBS gave the average mass density of  $2.6 \pm 0.1 \text{ g/cm}^3$  for the films. The given uncertainty is mainly due to differences in mass density between the samples.

According to the ESCA measurements the bonding ratio  $\text{sp}^3/\text{sp}^2$  was typically 70% for the DLC films. The observed average mass density of  $2.6 \pm 0.1 \text{ g/cm}^3$  relative to the density of diamond ( $3.51 \text{ g/cm}^3$ ) corresponds to the obtained amount of  $\text{sp}^3$  bonds.

Results of NRB measurement showed that hydrogen concentration was 0.07 at. % in the DLC films prepared in vacuum. Concentration distributions of the implanted hydrogen are illustrated in Fig. 1. In the calculation of the depth scale, the stopping powers for the probing N beam were taken from Ref. 20. The concentrations were deduced using a standard H-implanted Si sample in the NRB measurements.<sup>16</sup> The shape of the implanted H distribution after annealings at different temperatures was studied in two different sets of samples. The first set was implanted only with hydrogen. In the second set of samples He was implanted before H. This was done to find out if the damage created by He implantation has any influence on hydrogen trapping. As can be seen in the picture the depth profiles do not show any significant

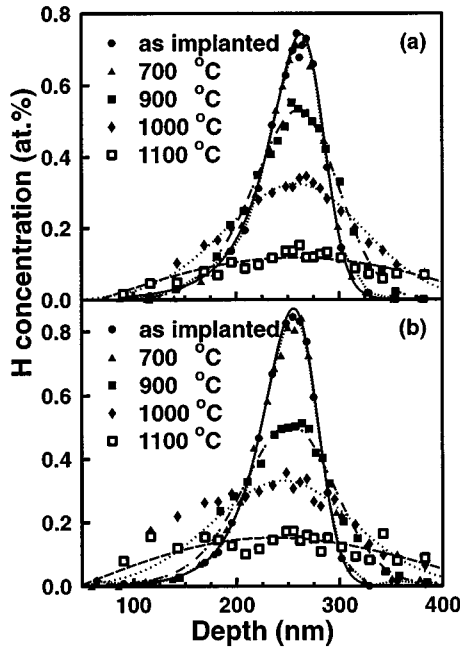


FIG. 1. Hydrogen concentration distributions observed in NRB measurements in  $H^+$  ion (a) and  $He^+$  and  $H^+$  ion (b) implanted samples. Distributions were observed after the implantation and after annealings at different temperatures. Solid line is the Pearson IV fit of the implanted depth profile. Dashed lines show the fitted diffusion profiles.

differences. In both cases hydrogen starts to migrate already at an annealing temperature of 700 °C. When the annealing temperature is increased the concentration profiles become broader and the maximum hydrogen concentration at the peak decreases. Hydrogen migrates in the course of annealings towards both the surface and bulk. The elastic-recoil-detection measurements show that no significant loss of H took place in the annealings.

Fig. 2 illustrates hydrogen concentration profiles measured with SIMS. The H concentration of the as-implanted hydrogen profile was normalized to the corresponding NRB profile. The relative sensitivity factor<sup>21</sup> to quantify hydrogen concentration in the annealed samples was calculated from the known H concentration in the as-implanted sample. Only

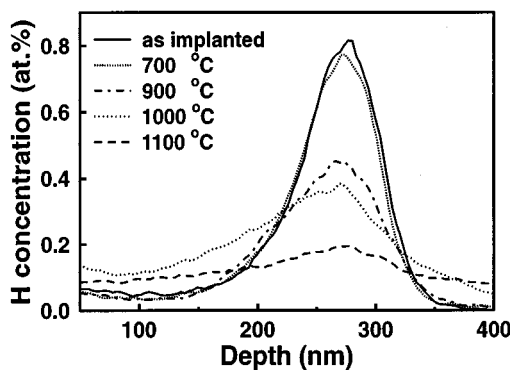


FIG. 2. Hydrogen concentration profiles after annealings at different temperatures obtained by SIMS.

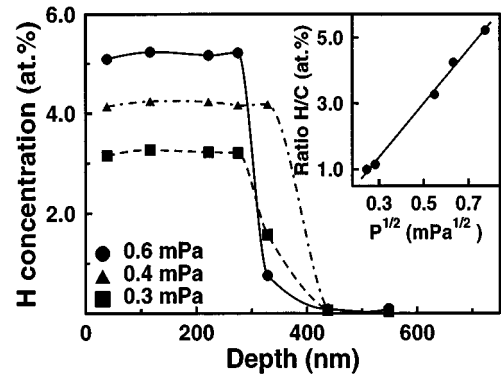


FIG. 3. Hydrogen concentration distributions observed in NRB measurements for DLC samples deposited in hydrogen atmosphere at different deposition pressures. The inset shows H concentration as a function of square root of the deposition pressure. Solid line is the linear fit of the experimental data.

hydrogen implanted samples were analyzed with SIMS. The full width at half maximum (FWHM) of the as-implanted SIMS profile is slightly higher than that of the NRB profile but otherwise the SIMS and NRB profiles are in agreement. In the annealed samples hydrogen starts to migrate at a temperature of 700 °C and in the course of annealings it diffuses towards bulk and surface. The annealed profiles are slightly broader than the corresponding NRB profiles. This is mainly due to longer annealing times in SIMS experiments.

H concentrations in the samples deposited in hydrogen atmosphere at different pressures were relatively constant throughout the film (Fig. 3). As can be seen in the figure, hydrogen content is proportional to the square root of the deposition pressure up to 0.6 mPa. Annealing experiments showed a decrease of the hydrogen concentration with increasing temperature, H release and migration to the interface (Fig. 4). It was observed that the release temperature varied between 950 and 1070 °C depending on the H concentration.

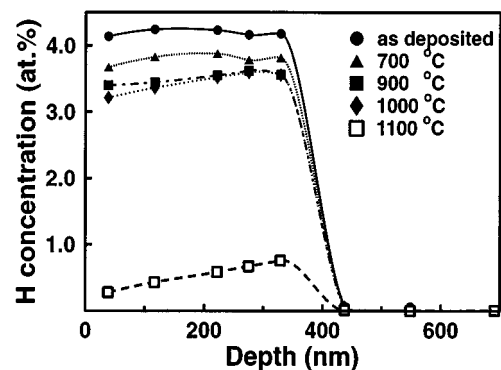


FIG. 4. Hydrogen concentration distribution observed in NRB measurements for DLC samples deposited in hydrogen atmosphere at a deposition pressure of 0.4 mPa. Distribution observed after the deposition and after annealings at different temperatures.

#### IV. ANALYSIS OF DIFFUSION

The Gaussian-like broadening of the H concentration profiles indicates a concentration independent diffusion with a solid solubility over 1 at. % at temperatures above 700 °C. For the deduction of the activation energy of H diffusion, the diffusion coefficients were calculated by solving numerically the one dimensional diffusion equation

$$\frac{\partial C}{\partial t} = D \frac{\partial^2 C}{\partial x^2}, \quad (1)$$

where  $C$  is the impurity concentration and  $D$  is the diffusion coefficient. A matrix method was used. By writing Eq. (1) as finite differences it is possible to get the concentration change for a time step  $\Delta t$ .

$$\Delta C = C_i^{t+\Delta t} - C_i^t = \frac{D\Delta t}{(\Delta x)^2} [(C_{i+1}^t - C_i^t) - (C_i^t - C_{i-1}^t)], \quad (2)$$

$$\begin{pmatrix} C_0^{t+\Delta t} \\ C_1^{t+\Delta t} \\ C_2^{t+\Delta t} \\ \vdots \\ C_n^{t+\Delta t} \end{pmatrix} = \begin{pmatrix} (1-2R) & R & 0 & 0 & 0 & \dots & 0 & 0 \\ R & (1-2R) & R & 0 & 0 & \dots & 0 & 0 \\ 0 & R & (1-2R) & R & 0 & \dots & 0 & 0 \\ \vdots & \vdots \\ 0 & 0 & 0 & 0 & \dots & 0 & R & (1-2R) \end{pmatrix} \begin{pmatrix} C_0^t \\ C_1^t \\ C_2^t \\ \vdots \\ C_n^t \end{pmatrix}. \quad (5)$$

$\Delta x$  and  $R$  were chosen to be 2 nm and 0.25, respectively. The corresponding time increment  $\Delta t$  can be calculated from Eq. (3) giving the ratio of diffusion time to  $\Delta t$  as the total number of matrix multiplications to obtain one solution. The diffusion coefficient for every temperature was determined by least squares fitting. The fitting was done by searching for diffusion coefficient used in Eq. (3) and by employing Eq. (5) until the best fit to the annealed curve was obtained.

Fig. 1 shows hydrogen concentration distributions observed in NRB measurements in H<sup>+</sup> ion implanted samples (a) and He<sup>+</sup> with H<sup>+</sup> implanted samples (b). The as-implanted, annealed at 700, 900, 1000, and 1100 °C profiles together with corresponding numerical fits are depicted.

The results presented in Fig. 5 show excellent Arrhenius behavior with the following values for the activation energy  $E_a$  and pre-exponential factor  $D_0$ :  $E_a = 2.1 \pm 0.1$  eV,  $D_0 = 1.3 \times 10^8$  nm<sup>2</sup>/s for DLC films implanted with H and  $E_a = 2.0 \pm 0.1$  eV,  $D_0 = 5.1 \times 10^7$  nm<sup>2</sup>/s for DLC films implanted with He and H. The activation energy and pre-exponential factor obtained from SIMS experiments for H implanted samples are  $E_a = 2.0 \pm 0.1$  eV and  $D_0 = 7.1 \times 10^7$  nm<sup>2</sup>/s, respectively. The results obtained with different methods are in a good agreement which allows us to conclude that the initial He implantation with the dose  $1 \times 10^{16}$  at./cm<sup>2</sup> does not influence the diffusion process. The effect of the probing <sup>15</sup>N beam on the H diffusion was checked by repeat-

ing the measurements at least two times. No significant effect was observed.

$$R = \frac{D\Delta t}{(\Delta x)^2}, \quad (3)$$

where  $C_i^t$  is the concentration at the depth  $x_i$  at time  $t$  and  $C_i^{t+\Delta t}$  is the concentration at time  $t + \Delta t$ .  $C_{i-1}^t$  and  $C_{i+1}^t$  are the concentrations at depths  $x_{i-1}$  and  $x_{i+1}$ , respectively. By defining a dimensionless variable

$$C_i^{t+\Delta t} = RC_{i-1}^t + (1-2R)C_i^t + RC_{i+1}^t, \quad (4)$$

and by isolating the concentration at the depth  $x_i$  at the time  $t + \Delta t$ , Eq. (2) can be rewritten as

which reads in matrix notation

ing the measurements at least two times. No significant effect was observed.

#### V. DISCUSSION

Since there are no data available in the literature on hydrogen diffusion in DLC films, we compare our results to the data on hydrogen diffusion in graphite and diamond. This illustrates differences in diffusivity of hydrogen in these different allotropic forms of carbon. The published results from the experimental and theoretical studies are somewhat controversial. Morita *et al.*<sup>22</sup> determined diffusion constants of implanted hydrogen in graphite in the temperature range from 200 to 600 °C. When their results are extrapolated to 700 °C the diffusion constant is approximately two orders of magnitude higher than our result. In addition to this, the presented activation energy, 0.20 eV, is very small. The diffusion constant of tritium in graphite has been studied by several authors.<sup>23,24</sup> They obtained activation energies for diffusion which were in the range from 1 to 2.7 eV at temperatures above 700 °C. Our value falls within this range, whereas the one obtained by Morita *et al.* is markedly smaller.

Recently Mehandru *et al.*<sup>25</sup> studied binding and diffusion of hydrogen in diamond. It was suggested that there are two pathways for H migration in the diamond lattice. Investigations were done using the semiempirical atom superposition and electron delocalization molecular orbital (ASED-

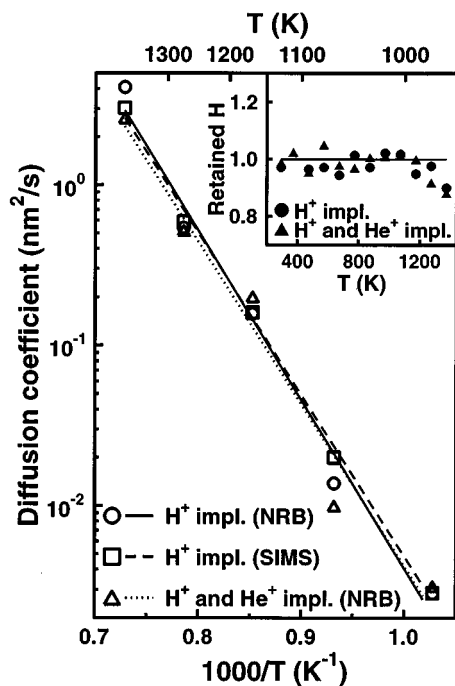


FIG. 5. Arrhenius plot for diffusion coefficient. Shown are the natural logarithms of the diffusion coefficients vs  $1000/T$ . The solid and the dashed lines show the fits in the case of  $H^+$  ion implanted samples measured by NRB and SIMS, respectively. The dot line is the fit in the case of  $He^+$  and  $H^+$  ion implanted sample. The inset shows that the ratio of retained H amount to the implanted H dose is constant in the temperature region used.

MO) theory. In the first path, the bond-centered (BC) hydrogen first travels to a neighboring tetrahedral (T) site and subsequently passes through the neighboring hexagonal and tetrahedral sites. The barrier for H moving from the BC site to the T site is calculated to be 5.3 eV. This value is equal to the energy difference between the BC- and T- localized hydrogen atoms. The T site was not a local energy minimum in those calculations. The second pathway for H migration involves the motion from the BC site to a similar neighboring site using the high density (110) planes. The calculated barrier for this case is 1.9 eV, which is lower than that for the first path. Thus theoretical calculations favor H migrating from one BC site to the next without the involvement of tetrahedral or hexagonal sites. For a more detailed description of the ASED-MO theory and calculation method, the reader is referred to an earlier work.<sup>25</sup> Theoretical investigations give the value for activation energy which is close to that obtained from the experimental data in the present work.

A rough approximation for H diffusion coefficient in type IIa natural diamond at 860 °C has been obtained to be 24 nm<sup>2</sup>/s by Popovici *et al.*<sup>10</sup> In their experiment, diffusion took place in a hydrogen atmosphere (pressure 4.0 kPa) under conditions specific to chemical vapor deposition (CVD) diamond growth. In this work, the diffusion coefficient is 0.7 nm<sup>2</sup>/s at 860 °C. So drastic a difference in the values of the diffusion coefficient can be partly due to a possible difference between natural diamond and PVD grown DLC film, the different diffusion conditions and the influence of the

surface hydrogen in the measurements of Ref. 10. The most probable explanation for so high a diffusion coefficient in the experiments of Popovici *et al.*<sup>10</sup> is that the diffusion temperature was not known. The temperature of a graphite support was measured and assigned to be the diffusion temperature. The diamond sample of 3 mm thickness was placed on the support, whereas the distance between the diamond surface and a 2100 °C hot filament placed in front of the sample was only 1 mm. Obviously the surface temperature was much higher than that for the sample support.

## VI. CONCLUSIONS

Properties of physical vapour deposited DLC films and migration of hydrogen in  $H^+$  and  $^4He^+$  ion implanted and hydrogen co-deposited DLC films have been studied using RBS, ESCA, PIXE, SIMS and NRB techniques. The films have a mass density of  $2.6 \pm 0.1$  g/cm<sup>3</sup> and the bonding ratio  $sp^3/sp^2$  is typically 70%. The films were annealed in vacuum at temperatures between 100 and 1100 °C. In the hydrogen co-deposited samples, hydrogen migrates towards the interface between the film and substrate and the overall amount of hydrogen decreases as a function of annealing temperature. In the case of implanted samples the migration of hydrogen is described well with a concentration independent diffusion equation. The diffusion coefficients exhibit a good Arrhenius behavior with an activation energy of  $2.0 \pm 0.1$  eV. Co-implantation with He did not have any significant effect on the diffusion of hydrogen.

## ACKNOWLEDGMENTS

This work was supported by the Association Euratom-TEKES. The authors thank Markku Heinonen (University of Turku) for ESCA measurements. One of us (E. Vainonen) wants to thank Dr. Jyrki Räisänen for helpful discussions regarding PIXE experiments. Jukka Kolehmainen and Janne Partanen (DIARC-Technology Inc.) are gratefully acknowledged for the sample preparation.

- <sup>1</sup>H. Atsumi, S. Tokura, and M. Miyake, *J. Nucl. Mater.* **155–157**, 241 (1988).
- <sup>2</sup>W. R. Wampler, B. L. Doyle, R. A. Causey, and K. L. Wilson, *J. Nucl. Mater.* **176,177**, 983 (1990).
- <sup>3</sup>J. W. Davis and A. A. Haasz, *J. Nucl. Mater.* **183**, 229 (1991).
- <sup>4</sup>S. Chiu and A. A. Haasz, *J. Nucl. Mater.* **196–198**, 972 (1992).
- <sup>5</sup>Y. Muto and K. Morita, *J. Nucl. Mater.* **223**, 262 (1995).
- <sup>6</sup>D. K. Avasthi, *Vacuum* **47**, 1249 (1996).
- <sup>7</sup>T. Sharda, D. S. Mirsa, and D. K. Avasthi, *Vacuum* **47**, 1259 (1996).
- <sup>8</sup>M. Malhotra, T. Som, V. N. Kulkarni, and S. Kumar, *Vacuum* **47**, 1265 (1996).
- <sup>9</sup>D. C. Ingram, J. C. Keay, and C. Tang, *Diam. Relat. Mater.* **2**, 1414 (1993).
- <sup>10</sup>G. Popovici, R. G. Wilson, T. Sung, M. A. Prelas, and S. Khasawinah, *J. Appl. Phys.* **77**, 5103 (1995).
- <sup>11</sup>Manufacturer's statements.
- <sup>12</sup>A. Anttila, J. Räisänen, and R. Lappalainen, *Nucl. Instrum. Methods Phys. Res. B* **12**, 245 (1985).
- <sup>13</sup>P. Aarnio, M. Nikkinen, and J. Routti, Sampo90, Logion Oy, Helsinki (1990).
- <sup>14</sup>T. P. Thin and J. Leroux, *X-ray Spectr.* **8**, 85 (1979).
- <sup>15</sup>J. Saarihahti and E. Rauhala, *Nucl. Instrum. Methods Phys. Res. B* **64**, 734 (1992).
- <sup>16</sup>H. S. Whitlow, J. Keinonen, M. Hautala, and A. Hautojärvi, *Nucl. Instrum. Methods Phys. Res. B* **5**, 505 (1984).

- <sup>17</sup>P. Torri, J. Keinonen, and K. Nordlund, Nucl. Instrum. Methods Phys. Res. B **84**, 105 (1994).
- <sup>18</sup>P. Haussalo, J. Keinonen, U.-M. Jäske, and J. Sievinen, J. Appl. Phys. **75**, 7770 (1994).
- <sup>19</sup>M. Hakovirta, J. Salo, R. Lappalainen, and A. Anttila, Phys. Lett. A **205**, 287 (1995).
- <sup>20</sup>J. F. Ziegler, J. P. Biersack, and U. Littmark, in *The Stopping and Range of Ions in Solids* edited by J. F. Ziegler (Pergamon, New York, 1985), Vol. 1; J. F. Ziegler and J. P. Biersack, TRIM-95 computer code (private communication).
- <sup>21</sup>R. G. Wilson, F. A. Stevie, and C. W. Magee, in *Secondary Ion Mass Spectrometry A Practical Handbook for Depth Profiling* (Wiley, New York, 1989), pp. 2.3-2, 3.1-1.
- <sup>22</sup>K. Morita, K. Ohtsuka, and Y. Hasebe, J. Nucl. Mater. **162–164**, 990 (1989).
- <sup>23</sup>M. Saeki, J. Nucl. Mater. **131**, 32 (1985).
- <sup>24</sup>R. A. Causey, M. I. Baskes, and K. Wilson, J. Vac. Sci. Technol. A **4**, 1189 (1986).
- <sup>25</sup>S. P. Mehandru, A. B. Anderson, and J. C. Angus, J. Mater. Res. **7**, 689 (1992).